Contents lists available at ScienceDirect

Bioorganic Chemistry

Quinoline-sulfamoyl carbamates/sulfamide derivatives: Synthesis, cytotoxicity, carbonic anhydrase activity, and molecular modelling studies

Elmas Begum Cakmak [a], Belma Zengin Kurt [b,*], Dilek Ozturk Civelek [c], Andrea Angeli [d], Atilla Akdemir [e], Fatih Sonmez [f], Claudiu T. Supuran [d,*], Mustafa Kucukislamoglu [g]

[a] *Sakarya University, Institute of Natural Sciences, 54050 Sakarya, Turkey*
[b] *Bezmialem Vakif University, Faculty of Pharmacy, Department of Pharmaceutical Chemistry, 34093 Istanbul, Turkey*
[c] *Bezmialem Vakif University, Faculty of Pharmacy, Department of Pharmacology, 34093 Istanbul, Turkey*
[d] *Università degli Studi di Firenze, Dipartimento Neurofarba, Sezione di Scienze Farmaceutiche e Nutraceutiche, Via U. Schiff 6, 50019 Sesto Fiorentino, Florence, Italy*
[e] *Bezmialem Vakif University, Faculty of Pharmacy, Department of Pharmacology, Computer-aided Drug Discovery Laboratory, 34093 Istanbul, Turkey*
[f] *Sakarya University of Applied Sciences, Pamukova Vocational School, 54055 Sakarya, Turkey*
[g] *Sakarya University, Faculty of Arts and Science, Department of Chemistry, 54050 Sakarya, Turkey*

ARTICLE INFO

ABSTRACT

Carbonic anhydrase (CA) IX, and XII isoforms are known to be highly expressed in various human tissues and malignancies. CA IX is a prominent target for some cancers because it is overexpressed in hypoxic tumors and this overexpression leads to poor prognosis. Novel twenty-seven compounds in two series (sulfamoylcarbamate-based quinoline (**2a-2o**) and sulfamide-based quinoline (**3a-3l**)) were synthesized and characterized by means of IR, NMR, and mass spectra. Their inhibitory activities were evaluated against CA I, CA II, CA IX, and CA XII isoforms. 2-Phenylpropyl (N-(quinolin-8-yl)sulfamoyl)carbamate (**2m**) exhibited the highest hCA IX inhibition with the K_i of 0.5 μM. In addition, cytotoxic effects of the synthesized compounds on human colorectal adenocarcinoma (HT-29; HTB-38), human breast adenocarcinoma (MCF7; HTB-22), human prostate adenocarcinoma (PC3; CRL-1435) and human healthy skin fibroblast (CCD-986Sk; CRL-1947) cell lines were examined. The cytotoxicity results showed that **2j**, **3a**, **3e**, **3f** are most active compounds in all cell lines (HT-29, MCF7, PC3, and CCD-986Sk).

1. Introduction

Cancer is one the most common cause of death in the world. Multiple mutations and epigenetic changes facilitate both the proliferation and survival of tumor cells. The uncontrolled growth of malignant cells leads to a high rate of nutrient and oxygen consumption. Inadequate environments such as lack of oxygen (hypoxia) force tumor cells to initiate response mechanisms that support cell life and migration. Therefore, more than 70% of solid tumors have distinctively hypoxic microenvironments [1]. The energy produced by glycolysis is important for cancer cells to survive and multiply under hypoxic conditions. The inefficiency of glycolysis in ATP production causes an increase in glucose consumption in hypoxic tumors. To make up for this deficiency, genes encoding key proteins involved in angiogenesis (eg vascular endothelial growth factor, VEGF), glucose transport (GLUT), glycolysis (eg phosphofructokinase 1, PFK-1), the export of monocarboxylic acids are upregulated [2]. These genes include the genes encoding membrane-

bound isozymes of carbonic anhydrase (CA), namely CA IX and CA XII [3]. CA IX is the most potent overexpressed gene in human cancer cells in response to hypoxia [4]. CA IX catalyzes the reversible conversion of carbon dioxide and thus plays a crucial role in stabilizing the extracellular pH by protecting cancer cells from apoptosis under hypoxia. It has been shown to have a similar overexpression profile for CA XII [5]. Physiologically, CA IX is present only with low expression in a small group of normal tissues such as gastric mucosa epithelium, small intestine epithelium, and gall bladder. However, overexpression of CA IX has been reported in many malignancies, including lung cancer, colon cancer, breast cancer, cervical cancer, renal cell carcinoma, and bladder cancer [6].

In general, carbonic anhydrases (CAs, EC 4.2.1.1) reversibly catalyze the hydration of CO_2 to bicarbonate and protons in all living organisms [7]. The 15 different α-CA isoforms identified in humans (h) differ by molecular features, some of such isoforms are cytosolic (CA I, CA II, CA III, CA VII, and CA XIII), others are membrane-bound (CA IV, CA IX, CA

XII, CA XIV, and CA XV), two of them are mitochondrial (CA VA and CA VB), and one isozyme is secreted in saliva (CA VI) [8,9]. These CA isoforms have been shown to play an active role in the mechanism of many diseases. Two cancer-associated CA isoforms IX and XII are actively involved in carbon dioxide metabolism, thus playing a role in pH control and tumor progression [5].

The first discovered molecules as CA inhibitors are the sulfonamides and their isoesters. Many researches have shown that unlike sulfonamide compounds, various compounds such as dithiocarbamates, xanthates, phenolics, polyamines, and coumarins act as CA inhibitors [10–13]. Recent studies show that (substituted) sulfamides, and sulfamoylcarbamates also exhibit some levels of CA inhibition [14–17]. The sulfamide moiety is structurally similar to those of sulfonamide and sulfamate, providing compounds bearing this structure to show a low nanomolar affinity for the target enzymes for which they were designed. This is achieved by the fact that the free or substituted sulfamide moiety plays an important role in binding to the active site of the inhibitor. The ability of the sulfamide group to give physicochemical properties similar to drug molecules to the organic structures to which they are attached, due to their properties such as increasing water solubility or showing better bioavailability, provides an advantage to the sulfamide group [18–20]. Quinoline is a skeleton that is widely used in medicinal chemistry. Quinoline derivatives have various biological and pharmacological activities, such as antimalarial, antifungal, antibacterial, antileishmanial and anticancer [21–25].

The approval of tumor-bound CA IX and XII, belonging to the family of carbonic enzymes, as antitumor drug targets have created a good research area for the synthesis of effective inhibitors of these enzymes. This study aimed to investigate the synthesis of new quinoline derivatives of bearing sulfamide/sulfamoylcarbamate and the biological activities of these compounds, which may be effective inhibitors of CAs. Their effects on CA I, CA II, CA IX, and CA XII isoforms, and cytotoxic properties on the HT-29, MCF7, PC3, and CCD-986Sk cell lines were evaluated. Furthermore, molecular modeling studies were performed to suggest possible modes of binding of these inhibitors inside the active sites of hCAs.

2. Result and discussion

2.1. Chemistry

In this study, two quinoline series (sulfamoylcarbamate-based quinoline (**2a-2o**) and sulfamide-based quinoline (**3a-3l**) derivatives) were synthesized.

The synthesis of first series consists of the reaction of various alcohols with chlorosulfonyl isocyanate (**1**). The alcohols were mixed with **1** in CH_2Cl_2 at 0 °C [26] and added 8-amino quinoline with Et_3N [27] to obtain **2a-2o** (Scheme 1).

The synthesis of second series consists of the reaction of sulfamoylcarbamate-based quinoline with various amine derivatives. The *tert*-butyl(*N*-(quinolin-8-yl)sulfamoyl)carbamate (**2a**) obtained by above method used *tert*-butylalcohol was reacted with 1° or 2° amine derivatives in THF at 60 °C [28] to give sulfamide-based quinoline (**3a-3l**) derivatives (Scheme 2).

All of the newly synthesized compounds were characterized by ^1H NMR, ^{13}C NMR, IR and MS. According to the IR spectra of the synthesized **2a-2o** and **3a-3l** derivatives, it was possible to observe the
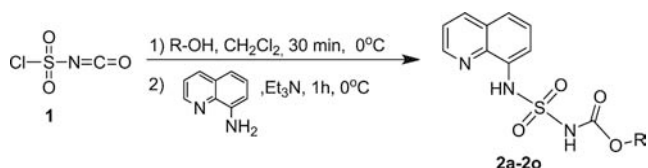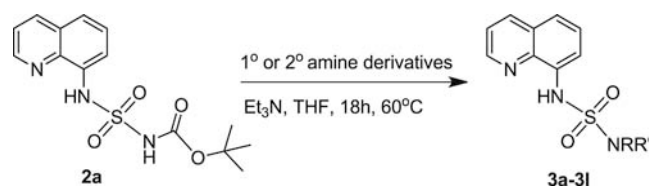
Scheme 2. Synthesis of new quinoline-sulfamide derivatives.

absorption at about 3200–3300 cm^{-1} relating to NH stretch of sulfamoyl or sulfamide groups. The stretch of the carbamate carbonyl moiety shows the absorbance between 1710 and 1740 cm^{-1}. From the ^1H NMR spectra; for the **2a-2o**; the signals for aromatic protons were observed between 7.36 and 9.77 ppm and aliphatic protons recorded about at 0.75–5.05 ppm. For the **3a-3l**; the signals for aromatic protons were observed between 6.31 and 8.73 ppm, NH proton signals detected about at 8.68–8.94 ppm, and aliphatic proton signals observed about at 0.59–5.73 ppm. From the ^{13}C NMR spectra, the signals of the 149 and 156 ppm can be seen for carbonyl of carbamate groups. The signals of the aliphatic and aromatic carbons were observed at 13–85 ppm and 114–154 ppm, respectively.

^1H NMR, ^{13}C NMR, and MS spectra of the synthesized compounds are given in supplementary materials.

2.2. CA inhibition

The CA inhibitory profiles of the synthesized compounds were evaluated by applying a stopped flow CO_2 hydrase assay [29], using acetazolamide (AAZ) as a standard inhibitor against four physiologically significant isoforms CA I, II, IX, and XII.
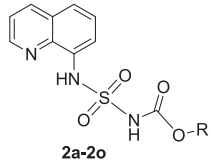
From the Table 1, the K_i values of the sulfamoylcarbamate-based quinolines (**2a-2o**) were determined in the range of 3.0 and > 100 μM, 0.6 and > 100 μM, 0.5 and > 100 μM, 6.9 and > 100 μM against hCA I, hCA II, hCA IX and hCA XII, respectively. hCA XII was inhibited weaker than other hCA isoforms (hCA I, hCA II, hCA IX). Among the first series, compound **2k** containing benzyl moiety showed the best inhibition of cytosolic isoform hCA I (associated with glaucoma) with K_i of 3.0 μM, which is close to that of AAZ (K_i of 0.25 μM) while compound **2g** bearing cycloheptyl moiety strongly inhibited the cytosolic isoform hCA II with K_i of 0.6 μM. hCA IX and hCA XII (tumor-associated isoforms) were inhibited by compound **2m** including phenylpropyl moiety with K_i of 0.5 μM and compound **2c** bearing pentyl group with K_i of 6.9 μM, respectively.

In addition, some notions about structure-activity relationship (SAR) observed from Table 1: (i) The cyclization of pentyl group strongly decreased the inhibitory activity against hCA XII (comparing **2c** (K_i = 6.9 μM) with **2e** (K_i = >100 μM)) and also the cyclization of hexyl group reduced the inhibitory activity almost 14-fold against hCA II (comparing **2d** (K_i = 5.5 μM) with **2f** (K_i = 74.3 μM)).

(ii) The presence of methylene between carbamate and *t*-butyl moieties dramatically decreased the inhibitory activity against hCA I, II, IX and XII (comparing **2a** (K_i values of 27.3 μM, 75.6 μM, 0.7 μM, 8.5 μM against hCA I, II, IX and XII, respectively) with **2b** (K_i values of >100 μM against all hCAs)). The similar effect was determined when compared **2l** (K_i values of 9.1 μM, 39.4 μM, 1.8 μM, 50.2 μM against hCA I, II, IX and XII, respectively) with **2n** (K_i values of >100 μM against all hCAs). In contrast, the presence of methylene between carbamate and phenyl raised the inhibitory activity against hCA I, II and XII (comparing **2j** (K_i values of 7.3 μM, 74.8 μM, and 81.5 μM, respectively) with **2k** (K_i values of 3.0 μM, 3.9 μM, and 22.5 μM, respectively)).

(iii) The methyl migration from β-position to α-position of carbamate moiety extremely reduced the all hCA inhibition (comparing **2m** (K_i values of 6.3 μM, 2.2 μM, 0.5 μM, 39.05 μM against hCA I, II, IX and XII, respectively) with **2n** (K_i values of >100 μM against all hCAs)). Furthermore, the methyl or phenyl binding to α-position of carbamate

Scheme 1. Synthesis of new sulfamoylcarbamate-based quinoline derivatives.

Table 1

In vitro inhibition K_i values of **2a-2o** for the hCA I, II, IX and XII.

2a-2o

Compound	R	Ki (μM)*			
		hCA I	hCA II	hCA IX	hCA XII
2a		27.3	75.6	0.7	8.5
2b		>100	>100	>100	>100
2c		3.7	7.2	0.6	6.9
2d		3.3	5.5	0.6	>100
2e		6.5	5.8	0.7	>100
2f		8.7	74.3	0.7	>100
2g		6.3	0.6	0.6	>100
2h		5.8	70.8	1.5	54.2
2i		>100	>100	>100	>100
2j		7.3	74.8	0.8	81.5
2k		3.0	3.9	0.8	22.5
2l		9.1	39.4	1.8	50.2
2m		6.3	2.2	0.5	39.0
2n		>100	>100	>100	>100
2o		>100	>100	>100	>100
AAZ	–	0.25	0.012	0.026	0.006

* Mean from 3 different assays, by a stopped flow technique.

Table 2

In vitro inhibition K_i values of **3a-3l** for the hCA I, II, IX and XII.

3a-3l

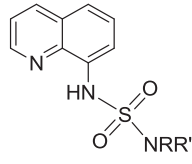| Compound	-NRR'	Ki (μM)*			
		hCA I	hCA II	hCA IX	hCA XII
3a		>100	>100	>100	>100
3b		>100	>100	>100	>100
3c		>100	>100	>100	>100
3d		>100	>100	>100	>100
3e		>100	>100	>100	>100
3f		7.9	56.4	0.7	8.5
3g		>100	>100	>100	>100
3h		>100	>100	>100	>100
3i		>100	>100	>100	>100
3j		>100	>100	>100	>100
3k		>100	>100	>100	>100
3l		>100	>100	>100	>100
AAZ	–	0.25	0.012	0.026	0.006

* Mean from 3 different assays, by a stopped flow technique.

moiety also decreased hCA I, II, IX and XII inhibitions ranging from almost 2-fold to 120-fold (comparing **2k** (K_i values of 3.0 μM, 3.9 μM, 0.8 μM and 22.5 μM, respectively) with **2l** (K_i values of 9.1 μM, 39.4 μM, 1.8 μM and 50.2 μM, respectively) and **2o** (K_i values of >100 μM against all hCAs)).

(iv) The ring expansion from cyclopentyl to cyclohexyl and cyclo-heptyl did not show linear and appreciable effect on hCA I, IX and XII inhibitions (comparing **2e** (K_i values of 6.5 μM, 0.7 μM and >100 μM, respectively) with **2f** (K_i values of 8.7 μM, 0.7 μM and >100 μM, respectively) and **2g** (K_i values of 6.3 μM, 0.6 μM and >100 μM, respectively)). On the other hand, hCA II inhibition was first decreased almost 13-fold, and then increased almost 120-fold by the ring expan-sion (comparing **2e** (K_i = 5.8 μM) with **2f** (K_i = 74.3 μM) and **2g** (K_i = 0.6 μM)).

From the Table 2, among the sulfamide-based compounds (**3a-3l**), only **3f** showed considerable inhibitory activity against all hCA isoforms. The others weakly inhibited the all hCAs (K_i values of >100 μM). The K_i values of the **3f** are 7.9 μM, 56.4 μM, 0.7 μM and 8.5 μM against hCA I, II,

IX and XII, respectively.

2.3. Cell viability against normal and cancer cell lines

Cell viability assay was carried out using human colorectal adeno-carcinoma (HT-29; HTB-38), human breast adenocarcinoma (MCF7; HTB-22), human prostate adenocarcinoma (PC3; CRL-1435) and human healthy skin fibroblast (CCD-986Sk; CRL-1947) cell lines. Each cell line was treated with the synthesized compounds for 48 h and 3-(4,5-dimethylthiazol-2-yl)-2,5-diphenyltetrazolium bromide (MTT) assay was used to determine the viability of cells. Doxorubicin (**dox**) was used as the reference compound. As shown in Table 3 **2j, 3a, 3e,** and **3f** are most active compounds against cancer cell lines. **3a, 3e** and **3f** are the most active compounds with the IC$_{50}$ values of 21.97 μM, 23.28 μM and 21.49 μM, respectively, against HT-29 cell line. The most cytotoxic compound against MCF7 cell line is **2j** with the IC$_{50}$ value of 12.75 μM. **3a** and **3f** are the most cytotoxic compounds with the IC$_{50}$ values of 14.77 μM and 12.10 μM, respectively, against PC3 cell line. The syn-thesized compounds were also tested in healthy cell line CCD-986Sk. It

Table 3

IC$_{50}$ values of the cytotoxicity of synthesized molecules at HT-29, MCF7, PC3, and CCD cell line.

Compound	IC$_{50}$ (μM)[*]			
	HT-29	MCF7	PC3	CCD
2a	205.3 ± 35.34	169.4 ± 27.09	236.1 ± 30.84	90.50 ± 15.13
2b	42.80 ± 6.04	27.37 ± 3.43	25.92 ± 3.39	22.39 ± 2.68
2c	305.9 ± 53.77	162.9 ± 14.22	88.83 ± 12.42	80.15 ± 13.02
2d	308.0 ± 53.53	191.1 ± 12.25	145.1 ± 20.53	118.7 ± 21.28
2e	231.0 ± 34.67	337.6 ± 53.06	106.9 ± 10.40	75.15 ± 13.49
2f	174.0 ± 33.35	269.7 ± 34.53	127.7 ± 17.51	85.58 ± 17.40
2g	393.5 ± 60.39	142.4 ± 14.04	51.18 ± 6.59	12.54 ± 1.75
2h	285.1 ± 22.51	116.1 ± 14.89	115.0 ± 12.68	61.31 ± 11.98
2i	311.2 ± 56.01	217.5 ± 42.43	89.63 ± 10.89	183.8 ± 41.12
2j	29.15 ± 3.08	12.75 ± 0.79	43.21 ± 5.98	32.31 ± 4.86
2k	352.5 ± 93.08	140.3 ± 10.95	231.3 ± 37.79	83.94 ± 14.80
2l	230.0 ± 44.65	112.8 ± 8.89	81.44 ± 5.74	69.54 ± 11.56
2m	243.9 ± 39.37	207.9 ± 29.69	91.86 ± 8.08	103.7 ± 22.11
2n	325.4 ± 36.15	155.6 ± 20.96	60.92 ± 7.18	68.99 ± 11.70
2o	275.8 ± 47.13	109.9 ± 11.39	84.05 ± 7.86	98.57 ± 19.39
3a	21.97 ± 3.45	19.82 ± 2.56	14.77 ± 2.30	15.09 ± 2.92
3b	81.12 ± 15.56	33.88 ± 5.26	84.02 ± 11.2	43.16 ± 7.51
3c	46.59 ± 9.70	37.33 ± 6.13	33.77 ± 4.87	27.56 ± 5.08
3d	32.44 ± 6.86	33.93 ± 3.92	39.84 ± 5.76	24.04 ± 5.92
3e	23.28 ± 3.82	19.81 ± 2.46	21.74 ± 3.01	13.23 ± 2.47
3f	21.49 ± 3.06	23.04 ± 3.56	12.10 ± 1.70	12.62 ± 2.13
3g	41.82 ± 7.95	50.13 ± 7.87	26.58 ± 4.20	32,36 ± 6,27
3h	43.27 ± 10.42	56.50 ± 10.41	30.90 ± 6.19	36.53 ± 8.04
3i	37.50 ± 6.26	23.83 ± 2.28	22.49 ± 3.26	19.69 ± 3.17
3j	290.3 ± 100.3	59.49 ± 6.77	50.21 ± 7.60	35.53 ± 6.20
3k	57.38 ± 7.65	45.82 ± 4.63	38.76 ± 4.53	36.28 ± 4.47
3l	443.1 ± 95.47	45.80 ± 4.34	105.8 ± 8.16	81.03 ± 20.35
dox	14.51 ± 3.65	0.46 ± 0.11	1.85 ± 0.41	0.16 ± 0.03

[*] The cell viability was represented as a percentage (%) relative to untreated cells as a control.

has been found that cytotoxicity results were almost similar against CCD-986Sk as the cancer cell lines. **2g**, **3a**, **3e**, and **3f** showed cytotoxic activity with the IC$_{50}$ values of 12.54 μM, 15.09 μM, 13.23 μM and 12.62 μM, respectively, against CCD-986Sk cell line.

2.4. Molecular modelling studies

Docking studies in combination with molecular dynamics simulations were conducted to suggest ligand-enzyme binding interactions for the (sulfamoylcarbamate-based quinoline (**2a-2o**) and sulfamide-based quinoline (**3a-3l**)) series with the active sites of the tumour-associated hCA IX and XII and the widely distributed hCA I and II. Binding interactions have been suggested for the sulfamoylcarbamates with the lowest K_i value for hCA I, IX and XII. No stable binding interaction has been obtained for the sulfamoylcarbamates in the hCA II active site. Also, no docked poses could be suggested for sulfamide derivatives that could explain the low K_i value for compound **3f** versus the high K_i values for the other members of the sulfamide series.

2.5. Suggested binding interactions of sulfamoylcarbamate series in the active sites of the tumour-associated hCA IX and XII

Compound **2m** shows the lowest measured K_i value among sulfamoylcarbamates (**2a-2o**) (K_i = 0.5 μM against hCA IX) with the exception of compounds **2b**, **2i**, **2n** and **2o** (Table 1). Nearly all compounds of the sulfamoylcarbamate series adopt a similar docked pose as **2m** (S-isomer) in the hCA IX active site. The quinolone ring is located between the sidechains of His94 and Leu198 and it may form H-arene interactions with the zinc-bound water molecule (Fig. 1). Both ligand NH functions could form hydrogen bonds with the backbone of Pro201 and one of the oxygen atoms of the sulfone group forms a hydrogen bond with the sidechain of Trp5, while the other oxygen atom is solvent exposed. Carbonyl group of the ligand forms a hydrogen bond with the

sidechain of Ser3. The substituents at position R1 points between the sidechain of Gln92 and Pro202 and may form hydrohobic interactions with the later residue. The R-isomer of the compounds adopts almost an identical pose in which only the methyl group changes its orientation. The ability of sulfamoylcarbamate series to adopt similar poses may explain the relatively narrow range of K_i values that have been obtained.

A 50 ns MD simulation was performed on the hCA IX – **2m** complex that was obtained from the docking study. The RMSD values of the binding pocket and protein (all heavy atoms) are generally below 2.5 Å during the entire simulation (Fig. 1). The RMSD value of the ligand first increases approximately to 6 Å and stays stable until 30 ns. After this point, the RMSD value increases again. From the ligand-protein interaction scheme it becomes clear that after 30 ns of MD simulation compound **2 m** does not form any interaction with the pocket anymore (Fig. 1**E**). During the first 30 ns of the simulation, compound **2m** forms frequently hydrogen bonds with the side chain of Trp5 and the backbone of Pro201 (Fig. 1**E**). In addition, hydrogen bonds have been observed with the sidechain (approximately 10–16 ns) and backbone (approximately 21–32 ns) of Gln2. Minor interaction are occassionaly observed with Ser3 (hydrogen bonds and H-arene interactions) and very few with Thr200 (hydrogen bonds) and Pro202 (H-arene interactions).

Interestingly, the calculated energy of binding suggests that the ligand binds with a similar energy between 6 and 50 ns of the MD simulation. In the later stages of the simulation, the ligand's sulfonamide group approaches the positively charged *N*-terminal of the protein (Glu0) and a hydrogen bond occurs. It should be noted that the hCA IX crystal structure is a truncated protein without the *N*-terminal transmembrane domain. As such, the hydrogen bond between ligand and the positively charged *N*-terminal of Glu0 is not considered of physiological importance.

The MD results suggest that the investigated hCA IX-**2m** complex does not form strong bonds and that compound **2m** may form multiple binding poses with either the investigated active site or allosteric sites.

The obtained docked poses of sulfamoylcarbamate series in the active site of hCA XII are more diverse compared to hCA IX. The poses are scattered throughout the pocket and there is no common pose found for the compounds. This may explain variation of measured K_i values.

The docked pose of compound **2c** (K_i = 6.9 μM against hCA XII) is shown in Fig. 2. Compound **2c** is located between Thr91 and Ser132 and forms hydrogen bonds with these residues. Again the sulfone group is solvent exposed.

A 50 ns MD simulation shows that the docked pose of **2c** changes significantly, especially after 4 ns and stays at approximately 6 Å until roughly 15 ns and then diminishes to 4 Å. At 20 ns the ligand RMSD value increases again to approximately 10–14 Å (Fig. 2). Hydrogen bonds are formed between the ligand in different poses and the sidechains of Lys67 and Gln92. The GBVI/WSA ligand-protein binding energy increased from −5 kcal/mol to approximately −3/−4 kcal/mol.

The MD simulation again suggests that **2c** may bind to the hCA XII active site with different poses, while allosteric sites cannot be excluded.

2.6. Docked poses of sulfamoylcarbamate series in the active sites of hCA I

The docked pose of compound **2k** (K_i = 3.0 μM against hCA I) in the active site of hCA I shows the presence of hydrogen bonds with the zinc-bound water molecule, and the side chains of His64, His67 and Gln92 (Fig. 3). In addition, hydrophobic interactions are observed with the sidechain of Phe91. All other compounds of sulfamoylcarbamates are able to adopt similar poses.

During a 50 ns MD simulation the RMSD of the ligand increases during the first nanosecond towards 4–5 Å, while the RMSD of the pocket and protein is between 1 and 2 Å. The GBVI/WSA binding energy changes from −5 kcal/mol to approximately −4 kcal/mol and fluctuates around this value. The ligand-protein interactions after the ligand reorientation in the first nanosecond stays stable and Hydrogen bonds
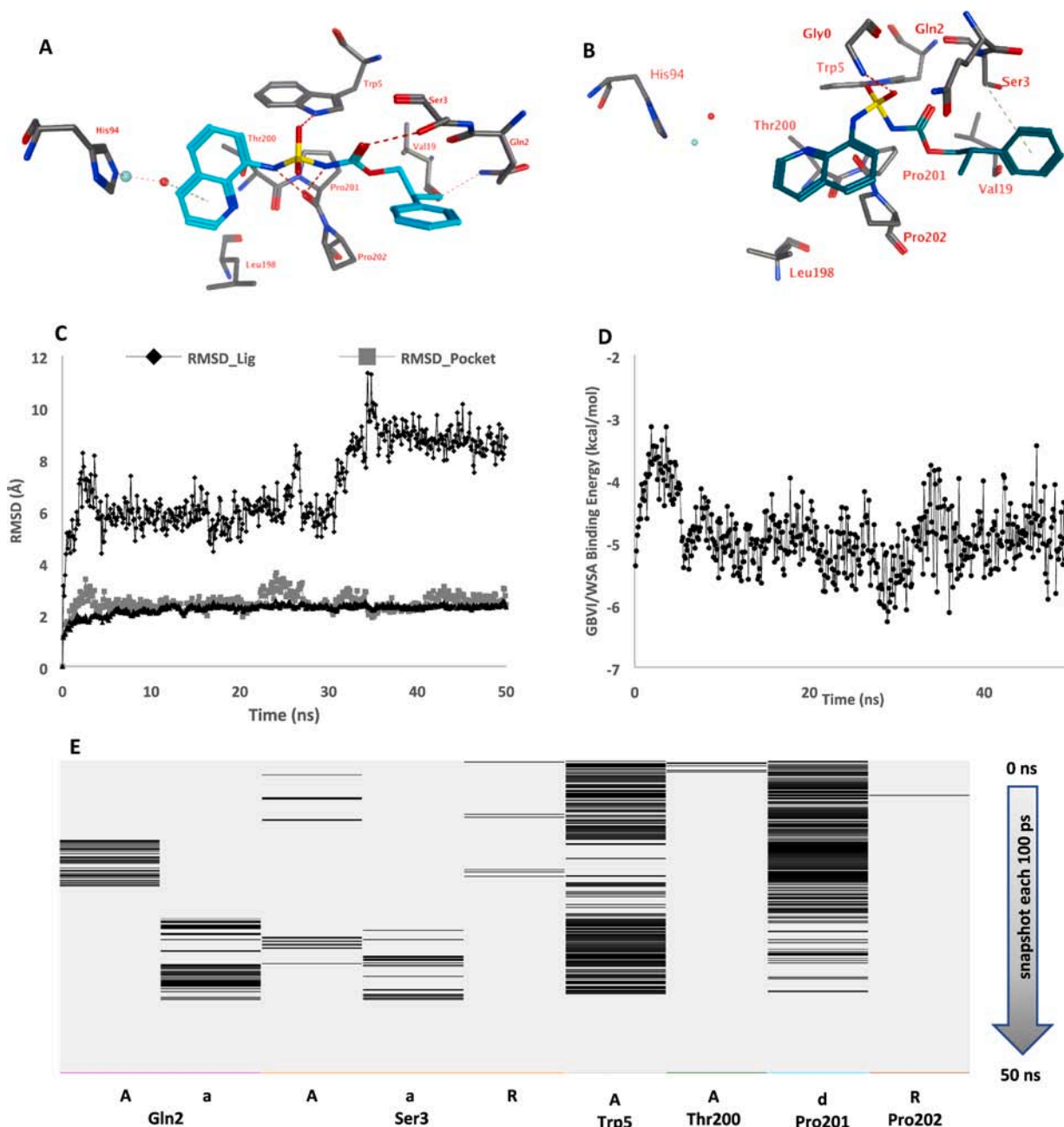
Fig. 1. A) The docked pose of compound **2m** in the active site of hCA IX. **B)** The pose after a 10 ns MD simulation. **C)** The RMSD values of ligand, pocket and protein. **D)** The GBVI/WSA energy of binding. **E)** The ligand-protein interactions. Hydrogen bonds and interactions with the zinc ion are indicated in red dashed lines and H-arene interactions are indicated in yellow dashed lines. The water molecule is indicated with a red sphere, while the zinc ion is indicated with a turquoise sphere. "a": backbone hydrogen bond acceptor interaction, "A": sidechain hydrogen bond acceptor interaction, "R": H-arene interaction and "d": backbone hydrogen bond donor interaction. (For interpretation of the references to colour in this figure legend, the reader is referred to the web version of this article.)

are frequently formed with the sidechains of His67 and Gln92.

The MD simulations indicate that compound **2k**, although flexible and dynamic, is able to constantly form hydrogen bonds with the hCA I active site.

3. Conclusion

The synthesis of new quinolone sulfamoylcarbamate and sulfamide derivatives and their inhibitory activity against four physiologically relevant CA isoforms, CA I (cytosolic isoform), CA II (associated with glaucoma and other pathologies), and CA IX and XII (tumor-associated isoforms) were evaluated. The effect of these compounds on the four different isoforms varied considerably. Sulfamoylcarbamates-based

quinoline (**2a-2o**) inhibited CA I, CA II, CA IX, and CA XII isoform at micromolar levels (except for **2b**, **2i**, **2n**, and **2o**), while only **3f** inhibited all CA isoforms at the micromolar level, among the sulfamide-based quinoline (**3a-3l**). These compounds were also evaluated in vitro on HT-29 human colorectal adenocarcinoma, MCF-7 human breast adenocarcinoma, PC3 human prostate adenocarcinoma, and CCD-986Sk human healthy skin fibroblast cell lines. The effect of these derivatives on four different cell lines varied according to the elements present in their molecular structure. **3a** and **3f** showed high cytotoxicity on the HT-29 cell line, whereas **2j** showed a higher cytotoxic effect on MCF7 cell line. Binding interactions between some of the hCAs have been investigated by computational methods, indicated that the possible ligand-enzyme interactions for each of the enzymes. The results showed that
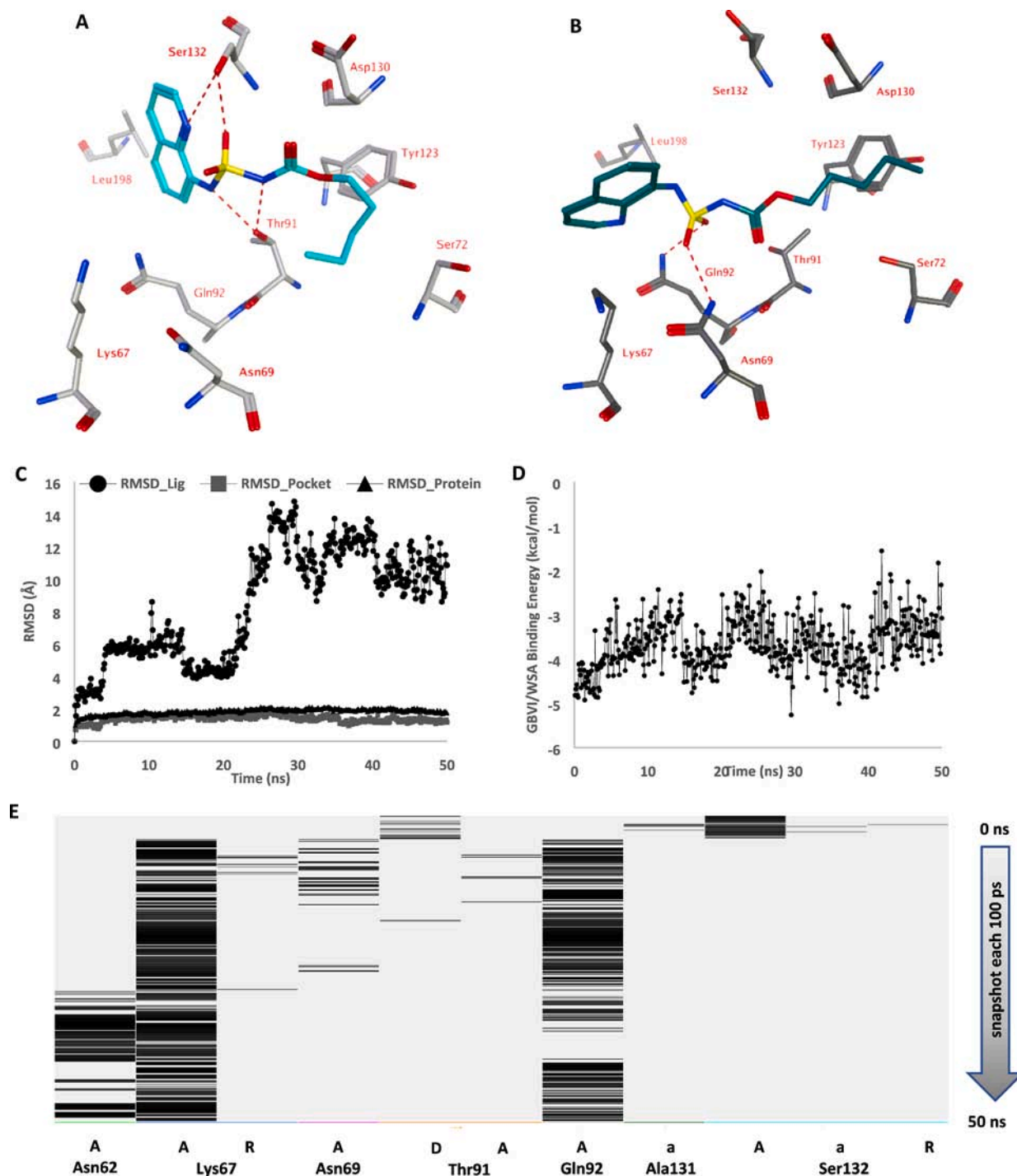
Fig. 2. (*A)* The docked pose of compound **2c** in the active site of hCA XII. **B)** The pose after a 10 ns MD simulation. **C)** The RMSD values of ligand, pocket and protein. **D)** The GBVI/WSA energy of binding. **E)** The ligand-protein interactions. Hydrogen bonds and interactions with the zinc ion are indicated in red dashed lines and H-arene interactions are indicated in yellow dashed lines. The water molecule is indicated with a red sphere, while the zinc ion is indicated with a turquoise sphere. "a": backbone hydrogen bond acceptor interaction, "A": sidechain hydrogen bond acceptor interaction, "R": H-arene interaction and "D": sidechain hydrogen bond donor interaction. (For interpretation of the references to colour in this figure legend, the reader is referred to the web version of this article.)

the sulfamoylcarbamates-based quinoline series are interesting molecules for CA inhibition and antiproliferative studies and most of them are more active than sulfamide-based quinoline against hCA I, II, IX and XII.

4. Experimental

4.1. Material and method

Melting points were taken on a STUART SMP40. IR spectra were measured on Alfa Bruker spectrometer.^{1}H and ^{13}C NMR spectra were measured on a Bruker spectrometer at 500 and at 125 Hz, respectively. [1]H and ^{13}C chemical shifts are referenced to the internal deuterated
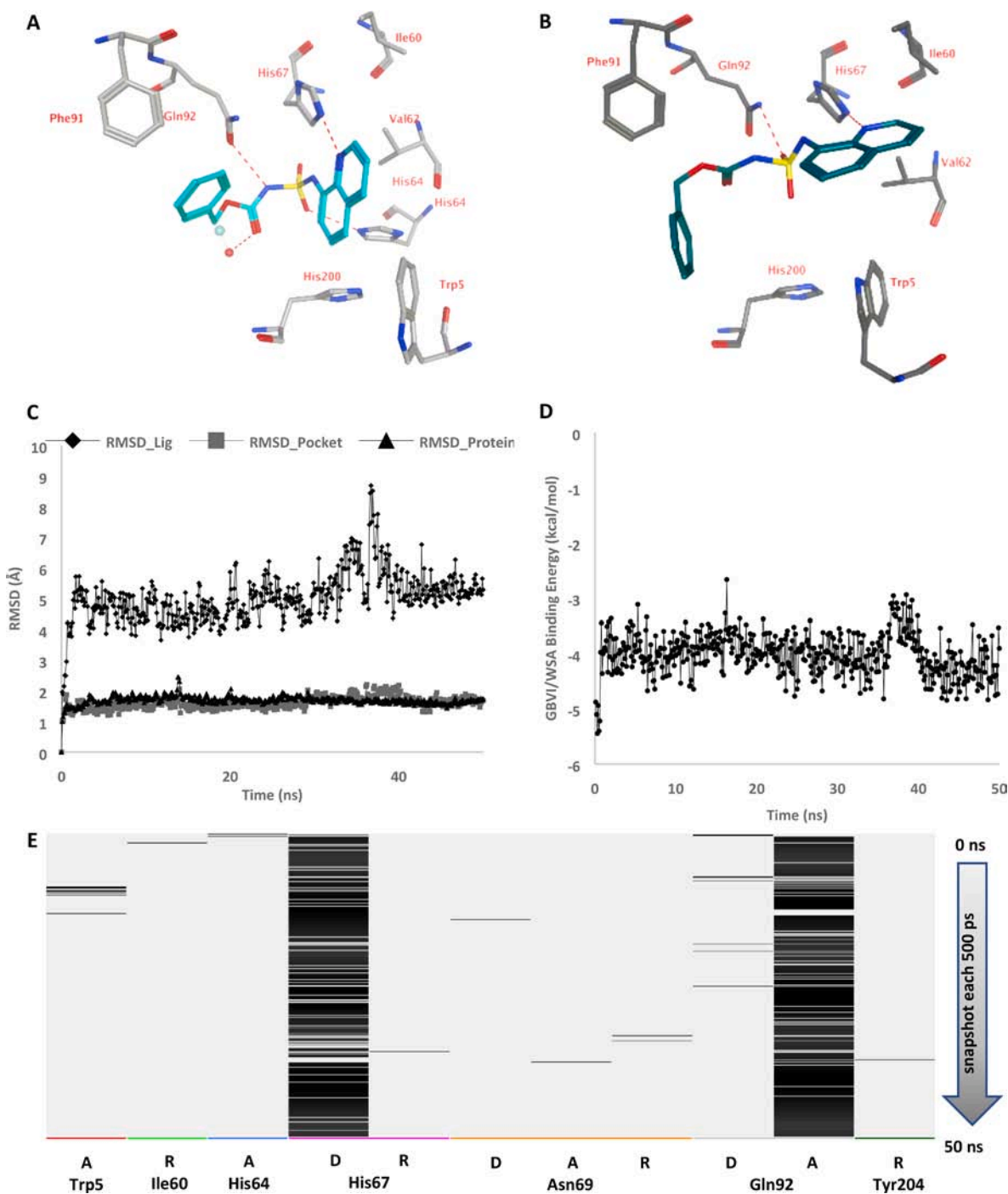
Fig. 3. **A)** The docked pose of compound **2k** in the active site of hCA I. **B)** The pose after a 10 ns MD simulation. **C)** The RMSD values of ligand, pocket and protein. **D)** The GBVI/WSA energy of binding. **E)** The ligand-protein interactions. Hydrogen bonds and interactions with the zinc ion are indicated in red dashed lines and H-arene interactions are indicated in yellow dashed lines. The water molecule is indicated with a red sphere, while the zinc ion is indicated with a turquoise sphere. "A": sidechain hydrogen bond acceptor interaction, "R": H-arene interaction and "D": sidechain hydrogen bond donor interaction. (For interpretation of the references to colour in this figure legend, the reader is referred to the web version of this article.)

solvent. Mass spectra were obtained using Thermo Fisher Scientific LC-HRMS spectrometer. Spectrophotometric analyses were performed by a BioTek Power Wave XS (BioTek, USA). The cell line was purchased from American Type Culture Collection (ATCC). Dulbecco's Modified Eagle's Medium-F12, RPMI Medium, fetal calf serum, and PBS were purchased from GIBCO BRL, InVitrogen (Carlsbad, CA). The chemicals and solvents were purchased from Fluka Chemie, Merck, Alfa Aesar and Sigma-Aldrich.

4.2. General procedures and spectral data

Synthesis of compounds 2a-2o: Chlorosulfonyl isocyanate (**1**) (1.2 mmol) and alcohol derivatives (1.2 mmol) were dissolved in dichloromethane (DCM) (5 mL), and the solution was stirred at 0 °C until 30 min [26]. It was then carefully added to a solution of 8-aminoquinoline (1.2 mmol) and triethylamine (1.2 mmol) in DCM at 0 °C and was stirred for 1 h. The mixture was concentrated in vacuo, and the residue was dissolved in EtOAc and washed with water and brine. The organic layer was

dried over MgSO$_4$ and concentrated under reduced pressure to give **2a-2o** [27]. The crude products were purified by column chromatography on silica gel from Hexan: Ethylacetate.

tert-butyl (*N*-(quinolin-8-yl)sulfamoyl)carbamate (**2a**): Whitish powder, 92% yield, mp. 120–121 °C; IR: 3133, 2990, 1714, 1509, 1476, 1369, 1327, 1150, 1058, 924, 826, 762, 589 cm^{-1}; ^{1}H NMR (CDCl$_3$, 500 MHz) δ/ppm: 8.85 (dd, *J* = 4.22, 1.64 Hz, 1H), 8.19 (dd, *J* = 8.29, 1.62 Hz, 1H), 7.82 (dd, *J* = 7.51, 1.30 Hz, 1H), 7.59 (dd, *J* = 8.29, 1.27 Hz, 1H), 7.54 (d, *J* = 7.59 Hz, 1H), 7.52–7.46 (m, 1H), 1.28 (s, 9H) ^{13}C NMR (CDCl$_3$, 125 MHz) δ/ppm: 149.0, 148.9, 138.4, 136.3, 133.2, 128.2, 127.0, 122.8, 122.1, 115.4, 84.3, 27.6; HRMS (ESI): C$_{14}$H$_{17}$N$_3$O$_4$S [M+Na]$^+$; calculated for 323.09, found 346,0830.

neopentyl (*N*-(quinolin-8-yl)sulfamoyl)carbamate (**2b**) White powder, 23% yield, mp. 108–109 °C; IR: 3200, 2956, 1743, 1503, 1453, 1414, 1381, 1316, 1235, 1157, 1087, 1058, 937, 878, 825, 793, 772, 758 cm^{-1}; ^{1}H NMR (CDCl$_3$, 500 MHz) δ/ppm: 8.75 (d, *J* = 3.24 Hz, 1H), 8.10 (d, *J* = 8.15 Hz, 1H), 7.74 (d, *J* = 7.38 Hz, 1H), 7.50 (d, *J* = 8.04 Hz, 1H), 7.46 (d, *J* = 7.71 Hz, 1H), 7.44–7.39 (m, 1H), 3.65 (m, 2H), 0.76 (s, 9H) ^{13}C NMR (CDCl$_3$, 125 MHz) δ/ppm: 156.4, 154.6, 142.9, 141.9, 138.2, 133.2, 131.9, 128.0, 127.8, 120.1, 79.5, 36.5, 30.8; HRMS (ESI): C$_{15}$H$_{19}$N$_3$O$_4$S [M+Na]$^+$; calculated for 337.11, found 360.0986.

pentyl (*N*-(quinolin-8-yl)sulfamoyl)carbamate (**2c**) Whitish powder, 37% yield, mp. 90–91 °C; IR: 3211, 3952, 2931, 1725, 1505, 1443, 1416, 1378, 1348, 1311, 1238, 1162, 1087, 929, 885, 825, 810, 795, 760, 657, 641 cm^{-1}; ^{1}H NMR (DMSO-*d*$_6$, 500 MHz) δ/ppm: 8.93 (d, *J* = 4.09 Hz, 1H), 8.46 (d, *J* = 8.34 Hz, 1H), 7.76 (d, *J* = 8.15 Hz, 1H), 7.70–7.62 (m, 3H), 3.92 (t, *J* = 6.68 Hz, 2H), 1.24–1.12 (m, 2H), 0.95–0.80 (m, 2H), 0.64–0.62 (m, 5H); ^{13}C NMR (CDCl$_3$, 125 MHz) δ/ppm: 150.5, 148.9, 138.3, 136.3, 133.1, 128.2, 126.9, 122.7, 122.2, 114.9, 65.7, 36.9, 24.6, 22.5, 22.3; HRMS (ESI): C$_{15}$H$_{19}$N$_3$O$_4$S [M+Na]$^+$; calculated for 337.11, found 360.0987.

hexyl (*N*-(quinolin-8-yl)sulfamoyl)carbamate (**2d**) Yellow powder, 26% yield, mp. 119–120 °C; IR: 3230, 2930, 2854, 1728, 1504, 1451, 1415, 1375, 1343, 1240, 1113, 1088, 941, 872, 848, 826, 795, 793, 630 cm^{-1}; ^{1}H NMR (CDCl$_3$, 500 MHz) δ/ppm: 8.78 (d, *J* = 4.19 Hz, 1H), 8.13 (d, *J* = 8.27 Hz, 1H), 7.75 (d, *J* = 7.49 Hz, 1H), 7.53 (d, *J* = 8.02 Hz, 1H), 7.48 (d, *J* = 7.68 Hz, 1H), 7.46–7.42 (m, 1H), 3.97 (t, *J* = 6.75 Hz, 2H), 1.58–1.52 (m, 2H), 1.46–1.09 (m, 6H), 0.78–0.75 (t, *J* = 6.92 Hz, 3H); ^{13}C NMR (CDCl$_3$, 125 MHz) δ/ppm: 150.5, 148.9, 138.4, 136.2, 133.1, 128.2, 126.8, 122.7, 122.2, 114.9, 67.3, 31.2, 28.2, 25.1, 22.4, 13.9; HRMS (ESI): C$_{16}$H$_{21}$N$_3$O$_4$S [M+Na]$^+$; calculated for 351.13, found 374.1143.

cyclopentyl (*N*-(quinolin-8-yl)sulfamoyl)carbamate (**2e**) Whitish powder, 35% yield, mp. 129–130 °C; IR: 3239, 2957, 2872, 1720, 1504, 1455, 1434, 1415, 1384, 1342, 1312, 1236, 1154, 1087, 926, 893, 827, 795, 773 cm^{-1}; ^{1}H NMR (CDCl$_3$, 500 MHz) δ/ppm: 8.77 (dd, *J* = 4.22, 1.61 Hz, 1H), 8.12 (dd, *J* = 8.29, 1.57 Hz, 1H), 7.75 (dd, *J* = 7.34, 1.44 Hz, 1H), 7.49 (dd, *J* = 8.27, 1.42 Hz, 1H), 7.46 (d, *J* = 7.40 Hz, 1H), 7.44–7.40 (m, 1H), 5.05–4.85 (m, 1H), 1.64–1.60 (m, 2H), 1.58–1.51 (m, 4H), 1.45–1.42 (m, 2H); ^{13}C NMR (CDCl$_3$, 125 MHz) δ/ppm: 150.2, 148.9, 138.3, 136.3, 133.1, 128.2, 126.9, 122.7, 122.2, 114.9, 80.8, 32.3, 23.4; HRMS (ESI): C$_{15}$H$_{17}$N$_3$O$_4$S [M+Na]$^+$; calculated for 335, found 358.0829.

cyclohexyl (*N*-(quinolin-8-yl)sulfamoyl)carbamate (**2f**) Yellow powder, 71% yield, mp. 122–123 °C; IR: 3293, 3260, 2931, 2851, 1747, 1505, 1431, 1381, 1315, 1223, 1150, 1006, 952, 930, 872, 751, 609 cm^{-1}; ^{1}H NMR (CDCl$_3$, 500 MHz) δ/ppm: 8.76 (dd, *J* = 4.2, 1.6 Hz, 1H), 8.11 (dd, *J* = 8.2, 1.5 Hz, 1H), 7.74 (dd, *J* = 7.50, 1.23 Hz, 1H), 7.50 (dd, *J* = 8.27, 1.16 Hz, 1H), 7.49–7.37 (m, 2H), 4.66–4.36 (m, 1H), 1.64–1.47 (m, 4H), 1.11–1.24 m, 6H); ^{13}C NMR (CDCl$_3$, 125 MHz) δ/ppm: 150.0, 148.9, 138.3, 136.3, 133.1, 128.2, 126.9, 122.7, 122.2, 115.0, 31.0, 25.1, 23.2; HRMS (ESI): C$_{16}$H$_{19}$N$_3$O$_4$S [M+Na]$^+$; calculated for 349.11, found 372.0985.

cycloheptyl (*N*-(quinolin-8-yl)sulfamoyl)carbamate (**2g**) Whitish powder, 27% yield, mp. 144–145 °C; IR: 3247, 3170, 2924, 2859, 1705, 1504, 1459, 1414, 1374, 1311, 1236, 1168, 1085, 928, 864, 823, 792, 758, 726, 609 cm^{-1}; ^{1}H NMR (DMSO-*d*$_6$, 500 MHz) δ/ppm: 8.93 (dd, *J* = 4.2, 1.5 Hz, 1H), 8.46 (dd, *J* = 8.3, 1.5 Hz, 1H), 7.76 (dd, *J* = 8.1, 1.1 Hz, 1H), 7.75–7.62 (m, 3H), 4.71–4.49 (m, 1H), 1.60–1.48 (m, 2H), 1.44–1.29 (m, 7H), 1.17–1.27 (m 3H); ^{13}C NMR (CDCl$_3$, 125 MHz) δ/ppm: 150.1, 148.9, 138.3, 136.3, 133.1, 128.2, 126.9, 122.7, 122.2, 115.0, 79.0, 33.2, 28.1, 22.4; HRMS (ESI): C$_{17}$H$_{21}$N$_3$O$_4$S [M+Na]$^+$; calculated for 363.13, found 386.1143.

adamantan-1-yl (*N*-(quinolin-8-yl)sulfamoyl)carbamate (**2h**) Yellow powder, 28% yield, mp. 237–238 °C; IR: 3172, 2906, 2853, 1739, 1503, 1450, 1410, 1373, 1317, 1228, 1148, 1086, 1035, 953, 868, 793, 759, 718, 628 cm^{-1}; ^{1}H NMR (CDCl$_3$, 500 MHz) δ/ppm: 8.80 (dd, *J* = 4.2, 1.6 Hz, 1H), 8.13 (dd, *J* = 8.2, 1.5 Hz, 1H), 7.76 (dd, *J* = 7.5, 1.2 Hz, 1H), 7.53 (dd, *J* = 8.28, 1.22 Hz, 1H), 7.48 (d, *J* = 7.61 Hz, 1H), 7.47–7.40 (m, 1H), 2.04–1.99 (m, 3H), 1.84 (d, *J* = 2.63 Hz, 6H), 1.52–1.46 (q, *J* = 12.50, 12.50, 12.50 Hz, 6H); ^{13}C NMR (CDCl$_3$, 125 MHz) δ/ppm: 148.8, 148.6, 138.4, 136.3, 133.3, 128.2, 127.0, 122.7, 122.1, 115.3, 84.2, 40.7, 35.8, 30.8; HRMS (ESI): C$_{20}$H$_{23}$N$_3$O$_4$S [M+Na]$^+$; calculated for 401.14, found 424, 1298.

2-isopropyl-5-methylcyclohexyl (*N*-(quinolin-8-yl)sulfamoyl)carbamate (**2i**) Yellow powder, 45% yield, mp. 155, 156 °C; IR: 3226, 3158, 2950, 1699, 1505, 1464, 1414, 1390, 1349, 1247, 1160, 1087, 932, 874, 825, 778, 767 cm^{-1}; ^{1}H NMR (CDCl$_3$, 500 MHz) δ/ppm: 8.63 (dd, *J* = 4.2, 1.6 Hz, 1H), 7.96 (dd, *J* = 8.3, 1.5 Hz, 1H), 7.57 (dd, *J* = 7.4, 1.2 Hz, 1H), 7.35 (dd, *J* = 8.2, 1.2 Hz, 1H), 7.31 (d, *J* = 7.5 Hz, 1H), 7.29–7.25 (m, 1H), 4.23 (dt, *J* = 10.9, 4.4 Hz, 1H), 1.42–1.28 (m, 3H), 1.22–1.17 (m, 1H), 1.13–0.93 (m, 2H), 0.72–0.59 (m, 1H), 0.51 (d, *J* = 6.7 Hz, 3H), 0.49–0.41 (m, 1H), 0.38 (d, *J* = 6.9 Hz, 3H), 0.13 (d, *J* = 6.93 Hz, 3H); ^{13}C NMR (CDCl$_3$, 125 MHz) δ/ppm: 150.0, 149.0, 138.2, 136.2, 133.2, 128.2, 126.8, 122.6, 122.2, 114.7, 46.8, 40.1, 33.8, 31.1, 25.8, 23.0, 21.8, 20.5, 15.7; HRMS (ESI): C$_{20}$H$_{27}$N$_3$O$_4$S [M+Na]$^+$; calculated for 405.17, found 428.1611.

phenyl (*N*-(quinolin-8-yl)sulfamoyl)carbamate (**2j**) White powder, 31% yield, mp. 176–177 °C; IR: 3284, 3220, 1738, 1666, 1536, 1503, 1491, 1470, 1319, 1163, 945 cm^{-1}; ^{1}H NMR (DMSO-*d*$_6$, 500 MHz) δ/ppm: 9.77 (s, 1H) 8.92 (dd, *J* = 4.2, 1.6 Hz, 1H), 8.87 (dd, *J* = 4.2, 1.6 Hz, 1H), 8.40 (dd, *J* = 8.3, 1.5 Hz, 1H), 8.39–8.34 (m, 1H), 8.25 (dd, *J* = 7.7, 1.1 Hz, 1H), 7.79 (dd, *J* = 7.5, 1.2 Hz, 1H), 7.71 (dd, *J* = 8.3, 1.1 Hz, 1H), 7.67–7.57 (m, 3H), 7.48 (d, *J* = 9.5, 6.4 Hz, 1H); ^{13}C NMR (DMSO-*d*$_6$, 125 MHz) δ/ppm: 156.4, 149.9, 148.4, 138.2, 137.0, 134.4, 133.6, 127.3, 123.1, 122.7, 122.2, 119.5, 115.5, 114.6; HRMS (ESI): C$_{16}$H$_{13}$N$_3$O$_4$S [M+H$_2$O+MeOH]$^+$; calculated for 393.41, found 393.2972.

benzyl (*N*-(quinolin-8-yl)sulfamoyl)carbamate (**2k**) Yellow powder, 64% yield, mp. 90–91 °C; IR: 3211, 2953, 2631, 2867, 1725, 1504, 1442, 1416, 1376, 1347, 1312, 1237, 1162, 1133, 1086, 930, 884, 795, 760, 657 cm^{-1}; ^{1}H NMR (CDCl$_3$, 500 MHz) δ/ppm: 8.69 (dd, *J* = 4.21, 1.48 Hz, 1H), 8.14 (dd, *J* = 8.29, 1.42 Hz, 1H), 7.75 (dd, *J* = 7.56, 1.05 Hz, 1H), 7.53 (dd, *J* = 8.27, 1.03 Hz, 1H), 7.47 (d, *J* = 7.79 Hz, 1H), 7.46–7.39 (m, 1H), 7.12–7.07 (m, 3H), 7.18–7.15 (m, 2H), 4.98 (s, 2H); ^{13}C NMR (CDCl$_3$, 125 MHz) δ/ppm: 150.5, 148.9, 138.3, 136.3, 133.1, 128.2, 126.9, 122.7, 122.2, 114.9, 65.7; HRMS (ESI): C$_{17}$H$_{15}$N$_3$O$_4$S [M+H]$^+$; calculated for 360.10, found 360.0987.

1-phenylethyl (*N*-(quinolin-8-yl)sulfamoyl)carbamate (**2l**) White powder, 25% yield, mp. 110–111 °C IR: 3243, 3217, 1737, 1594, 1504, 1450, 1436, 1414, 1383, 1344, 1312, 1232, 1162, 1135, 1087, 938, 836, 796, 754, 732, 698 cm^{-1}; ^{1}H NMR (DMSO-*d*$_6$, 500 MHz) δ/ppm: 8.86 (dd, *J* = 4.22, 1.61 Hz, 1H), 8.45 (dd, *J* = 8.33, 1.55 Hz, 1H), 7.77 (dd, *J* = 8.15, 1.16 Hz, 1H), 7.70 (dd, *J* = 7.61, 1.27 Hz, 1H), 7.66–7.62 (m, 2H), 7.20–7.12 (m, 3H), 7.11–7.05 (m, 2H), 5.59 (q, *J* = 6.5 Hz, 1H), 1.29 (d, *J* = 6.6 Hz, 3H); ^{13}C NMR (DMSO-*d*$_6$, 125 MHz) δ/ppm: 150.8, 149.9, 141.2, 137.3, 133.4, 128.6, 128.4, 127.8, 127.2, 126.0, 125.8, 123.4, 123.0, 115.5, 74.4, 22.2; HRMS (ESI): C$_{18}$H$_{17}$N$_3$O$_4$S C$_{17}$H$_{15}$N$_3$O$_4$S [M+Na]$^+$; calculated for 371.09, found 394.0831.

2-phenylpropyl (*N*-(quinolin-8-yl)sulfamoyl)carbamate (**2m**) White powder, 22% yield, mp. 111–112 °C IR: 3252, 2972, 2958, 2923, 1740, 1506, 1470, 1453, 1437, 1416, 1375, 1338, 1242, 1162, 926, 880, 825,

793, 757, 697 cm^{-1}; ^{1}H NMR (CDCl$_3$, 500 MHz) δ/ppm: 8.76 (dd, J = 4.08, 1.62 Hz, 1H), 8.11 (dd, J = 8.2, 1.5 Hz, 1H), 7.72 (dd, J = 7.56, 1.04 Hz, 1H), 7.52 (d, J = 8.2 Hz, 1H), 7.45 (d, J = 7.7 Hz, 1H), 7.4–7.04 (m, 1H), 7.14 (t, J = 7.30 Hz, 2H), 7.11–7.06 (m, 1H), 6.99 (d, J = 7.14 Hz, 2H), 4.03 (d, J = 7.49 Hz, 2H), 2.93–2.85 (m, 1H), 1.08 (d, J = 7.02 Hz, 3H); ^{13}C NMR (CDCl$_3$, 125 MHz) δ/ppm: 150.3, 149.0, 143.2, 142.2, 138.4, 136.2, 133.0, 128.5, 128.2, 127.3, 127.1, 126.8, 122.8, 122.2, 115.1, 71.6, 38.7, 17.5; HRMS (ESI): C$_{19}$H$_{19}$N$_3$O$_4$S C$_{17}$H$_{15}$N$_3$O$_4$S [M+Na]$^+$; calculated for 385.11, found 408.0986.

1-phenylpropan-2-yl (*N*-(quinolin-8-yl)sulfamoyl)carbamate (**2n**) White powder, 32% yield, mp. 107–108 °C; IR: 3272, 3209, 1721, 1508, 1442, 1415, 1379, 1312, 1242, 1150, 1090, 925, 884, 823, 756, 741, 705, 665, 650 cm^{-1}; ^{1}H NMR (CDCl$_3$, 500 MHz) δ/ppm: 8.74 (dd, J = 4.22, 1.60 Hz, 1H), 8.10 (dd, J = 8.30, 1.55 Hz, 1H), 7.73 (dd, J = 7.55, 1.18 Hz, 1H), 7.51 (dd, J = 8.27, 1.07 Hz, 1H), 7.44 (t, J = 7.7 Hz, 1H), 7.40 (dd, J = 8.28, 4.23 Hz, 1H), 7.09–7.00 (m, 3H), 6.95–6.87 (m, 2H), 4.89–4.83 (m, 1H), 2.69 (dd, J = 13.6, 6.0 Hz, 1H), 2.52 (dd, J = 13.66, 6.8 Hz, 1H), 0.95 (d, J = 6.31 Hz, 3H); ^{13}C NMR (CDCl$_3$, 125 MHz) δ/ppm: 156.6, 149.9, 149.0, 138.3, 136.3, 133.1, 129.5, 129.3, 128.3, 126.9, 126.6, 122.7, 122.2, 115.0, 75.1, 41.6, 18.8; HRMS (ESI): C$_{19}$H$_{19}$N$_3$O$_4$S [M+Na]$^+$; calculated for 385.11, found 408.0986.

benzhydryl (*N*-(quinolin-8-yl)sulfamoyl)carbamate (**2o**) Grey powder, 20% yield, mp. 138–139 °C; IR: 3251, 3096, 3033, 1730, 1483, 1455, 1416, 1386, 1228, 1159, 1090, 925, 878, 861, 769, 763, 744, 697, 610 cm^{-1}; ^{1}H NMR (DMSO-d_6, 500 MHz) δ/ppm: 8.75 (dd, J = 4.21, 1.59 Hz, 1H), 8.44 (dd, J = 8.33, 1.56 Hz, 1H), 7.77 (dd, J = 8.16, 1.05 Hz, 1H), 7.70 (dd, J = 7.61, 1.21 Hz, 1H), 7.66–7.58 (m, 2H), 7.35 (d, J = 4.36 Hz, 1H), 7.19–7.17 (m, 5H), 7.16–7.13 (m, 4H), 6.60 (s, 1H); ^{13}C NMR (DMSO-d_6, 125 MHz) δ/ppm: 150.6, 149.8, 140.0, 138.2, 137.1, 133.3, 128.8, 128.4, 128.2, 127.1, 126.9, 126.6, 123.3, 123.0, 115.4, 78.6; HRMS (ESI): C$_{23}$H$_{19}$N$_3$O$_4$S [M+Na]$^+$; calculated for 433.11, found 456.0986.

Synthesis of compounds 3a-3l: Chlorosulfonyl isocyanate (**1**) (1.2 mmol) and *t*-BuOH (1.2 mmol) were dissolved in dichloromethane (DCM) (5 mL), and the solution was stirred at 0 °C until 30 min. The mixture was then carefully added to a solution of 8-aminoquinoline (1.2 mmol) and triethylamine (1.2 mmol) in DCM at 0 °C and stirred for 1 h. The mixture was concentrated in vacuo, and the residue was dissolved in EtOAc and washed with water and brine. The organic layer was dried over MgSO$_4$ and concentrated under reduced pressure to give **2a**. **2a** (1.25 mmol), amine derivatives (1.25 mmol), and Et$_3$N (1.25 mmol) in THF were solved and stirred at 60 °C, 18 h. The solution was concentrated in vacuo, and the residue was dissolved in EtOAc and washed with water and brine. The organic layer was dried over MgSO$_4$ and concentrated under reduced pressure to give **3a-3l** [28]. The crude products were purified by column chromatography on silica gel from Hexan: Ethylacetate.

1,1-diethyl-N-(N-(quinolin-8-yl)sulfamide (**3a**) Grey powder, 30% yield, mp. 86–87 °C; IR: 3308, 2977, 2931, 2882, 1621, 1582, 1470, 1410, 1361, 1334, 1306, 1142, 1014, 924, 821, 785, 759, 687 cm^{-1}; ^{1}H NMR (CDCl$_3$, 500 MHz) δ/ppm: 8.84 (s, 1H), 8.66 (dd, J = 4.23, 1.66 Hz, 1H), 8.02 (dd, J = 8.29, 1.67 Hz, 1H), 7.62–7.52 (m, 1H), 7.42–7.34 (m, 2H), 7.36–7.29 (m, 1H), 3.21 (q, J = 7.17 Hz, 4H), 0.94–0.91 (t, J = 7.21 Hz, 6H); ^{13}C NMR (CDCl$_3$, 125 MHz) δ/ppm: 148.6, 138.3, 136.3, 134.5, 128.1, 126.8, 122.0, 121.4, 114.5, 42.0, 13.4; HRMS (ESI): C$_{13}$H$_{17}$N$_3$O$_2$S [M+Na]$^+$; calculated for 279.1041, found 302.0932.

propyl (quinolin-8-yl)sulfamide (**3b**) White powder, 34% yield, mp. 100–101 °C; IR: 3297, 2966, 2935, 2875, 1579, 1503, 1460, 1409, 1361, 1351, 1333, 1308, 1148, 1131, 1066, 1006, 931, 817, 789, 747 cm^{-1}; ^{1}H NMR (CDCl$_3$, 500 MHz) δ/ppm: 8.94 (s, 1H), 8.73 (dd, J = 4.20, 1.62 Hz, 1H), 8.09 (dd, J = 8.28, 1.63 Hz, 1H), 7.68 (dd, J = 8.88, 4.47 Hz, 1H), 7.44 (d, J = 4.36 Hz, 2H), 7.40 (dd, J = 8.28, 4.21 Hz, 1H), 4.78 (s, 1H), 2.90 (q, J = 6.89 Hz, 2H), 1.37–1.27 (m, 2H), 0.65 (t, J = 7.41 Hz, 3H); ^{13}C NMR (CDCl$_3$, 125 MHz) δ/ppm: 147.6, 137.2, 135.3, 133.2, 127.1, 125.9, 121.0, 120.5, 113.1, 43.9, 21.4, 9.9; HRMS (ESI): C$_{12}$H$_{15}$N$_3$O$_2$S [M+Na]$^+$; calculated for 265.0885, found 288.0775.

1,1-diisopropyl-N-(N-(quinolin-8-yl)sulfamide (**3c**) Grey powder, 40% yield, mp. 106–107 °C; IR: 3293, 2976, 2934, 1592, 1470, 1364, 1334, 1301, 1174, 1133, 1066, 1020, 966, 916, 879, 789, 673 cm^{-1}; ^{1}H NMR (CDCl$_3$, 125 MHz) δ/ppm: 8.88 (s, 1H), 8.69 (dd, J = 4.22, 1.64 Hz, 1H), 8.05 (dd, J = 8.28, 1.65 Hz, 1H), 7.76 (dd, J = 8.89, 4.45 Hz, 1H), 7.40–7.37 (m, 2H), 7.35–7.31 (m, 1H), 3.63–3.57 (m, 2H), 1.09 (d, J = 7.03 Hz, 12H); ^{13}C NMR (CDCl$_3$, 125 MHz) δ/ppm: 148.6, 138.5, 136.3, 134.5, 128.1, 126.8, 121.8, 121.5, 115.0, 48.8, 21.6; HRMS (ESI): C$_{15}$H$_{21}$N$_3$O$_2$S [M+Na]$^+$; calculated for 307.1354, found 330.1242.

butyl(N-(quinolin-8-yl)sulfamide (**3d**) Grey liquid, 38% yiled; IR: 3275, 2959, 2935, 2871, 1580, 1469, 1432, 1410, 1329, 1301, 1124, 1084, 1057, 917, 822, 790, 754, 653 cm^{-1}; ^{1}H NMR (CDCl$_3$, 500 MHz) δ/ppm: 8.94 (s, 1H), 8.73 (dd, J = 4.10, 1.33 Hz, 1H), 8.09 (dd, J = 8.27, 1.31 Hz, 1H), 7.68 (t, J = 4.40, 4.40 Hz, 1H), 7.44 (d, J = 4.43 Hz, 2H), 7.40 (t, J = 8.26, 3.98, 3.98 Hz, 1H), 4.73 (s, J = 5.55, 5.55 Hz, 1H), 2.94 (t, J = 20.11, 6.76, 6.76 Hz, 2H), 1.31–1.20 (m, 2H), 1.11–1.00 (m, 2H), 0.62–0.59 (t, J = 7.37, 7.37 Hz, 3H); ^{13}C NMR (CDCl$_3$, 125 MHz) δ/ppm: 148.7, 138.3, 136.3, 134.3, 128.2, 127.0, 122.0, 121.6, 114.2, 42.9, 31.1, 19.5, 13.4; HRMS (ESI): C$_{13}$H$_{17}$N$_3$O$_2$S [M+Na]$^+$; calculated for 279.1041, found 302.0933.

N-(quinolin-8-yl)pyrrolidine-1-sulfamide (**3e**) Brown powder, 43% yield, mp. 80–81 °C; IR: 3445, 3276, 2974, 1721, 1681, 1505, 1471, 1505, 1471, 1437, 1367, 1334, 1305, 1195, 1151, 1055, 1011, 913, 824, 792, 754 cm^{-1}; ^{1}H NMR (CDCl$_3$, 500 MHz) δ/ppm: 8.87 (s, 1H), 8.73 (dd, J = 4.19, 1.61 Hz, 1H), 8.09 (dd, J = 8.28, 1.62 Hz, 1H), 7.71 (dd, J = 5.51, 3.36 Hz, 1H), 7.47–7.41 (m, 2H), 7.39 (dd, J = 8.27, 4.19 Hz, 1H), 3.29–3.27 (m, 4H), 1.69–1.66 (m, 4H); ^{13}C NMR (CDCl$_3$, 125 MHz) δ/ppm: 148.6, 138.3, 136.3, 134.7, 128.2, 126.9, 121.9, 121.4, 114.7, 48.4, 25.5; HRMS (ESI): C$_{13}$H$_{15}$N$_3$O$_2$S [M+Na]$^+$; calculated for 277.0885, found 300.0777.

N-(quinolin-8-yl)piperidine-1-sulfamide (**3f**) Pink powder, 25% yield, mp. 128–129 °C; IR: 3245, 2943, 2846, 1581, 1411, 1373, 1339, 1308, 1278, 1159, 1089, 1054, 933, 920, 845, 823, 795, 766, 716 cm^{-1}; ^{1}H NMR (CDCl$_3$, 500 MHz) δ/ppm: 8.84 (s, 1H), 8.74 (dd, J = 4.19, 1.62 Hz, 1H), 8.14–8.06 (m, 1H), 7.70 (dd, J = 5.32, 3.56 Hz, 1H), 7.46–7.41 (m, 2H), 7.40 (dd, J = 8.25, 4.21 Hz, 1H), 3.21–3.15 (m, 4H), 1.44 (dd, J = 11.19, 5.51 Hz, 4H), 1.34 (dd, J = 9.60, 4.16 Hz, 2H); ^{13}C NMR (CDCl$_3$, 125 MHz) δ/ppm: 148.6, 138.3, 136.3, 134.7, 128.2, 126.9, 121.9, 121.3, 114.8, 47.2, 25.2, 23.5; HRMS (ESI): C$_{14}$H$_{17}$N$_3$O$_2$S [M+Na]$^+$; calculated for 291.1041, found 314.0931.

cyclohexyl (N-(quinolin-8-yl)sulfamide) (**3g**) White powder, 33% yield, mp. 133–134 °C; IR: 3274, 2935, 2857, 1504, 1470, 1414, 1363, 1305, 1164, 1058, 931, 885, 823, 794, 754, 657 cm^{-1}; ^{1}H NMR (CDCl$_3$, 500 MHz) δ/ppm: 8.75 (s, 1H), 8.70–8.63 (m, 1H), 8.11–7.96 (m, 1H), 7.56 (dd, J = 6.23, 2.32 Hz, 1H), 7.34–7.26 (m, 3H), 6.52 (s, 1H), 3.09 (s, 1H), 2.92 (s, 1H), 1.54–1.10 (m, 4H), 1.09–0.90 (m, 6H); ^{13}C NMR (CDCl$_3$, 125 MHz) δ/ppm: 148.4, 138.0, 136.2, 134.6, 128.0, 126.8, 121.8, 120.9, 113.7, 52.7, 39.9, 33.4, 24.7; HRMS (ESI): C$_{15}$H$_{19}$N$_3$O$_2$S [M+Na]$^+$; calculated for 305.1198, found 328.1089.

2-(cyclohex-1-en-1-yl)ethyl-(N-(quinolin-8-yl)sulfamide) (**3h**) White powder, 35% yield, mp. 87–88 °C; IR: 3306, 3266, 2932, 1503, 1472, 1415, 1326, 1306, 1137, 1082, 1064, 1025, 961, 921, 865, 823, 792, 759 cm-1; ^{1}H NMR (CDCl$_3$, 500 MHz) δ/ppm: 8.94 (s, 1H), 8.75 (dd, J = 4.21, 1.64 Hz, 1H), 8.10 (dd, J = 8.29, 1.64 Hz, 1H), 7.68 (dd, J = 6.32, 2.52 Hz, 1H), 7.45 (d, J = 1.99 Hz, 2H), 7.41 (dd, J = 8.23, 4.17 Hz, 1H), 5.14 (s, 1H), 4.54 (t, J = 5.46 Hz, 1H), 3.02–2.93 (m, 2H), 1.89 (t, J = 6.29, 6.29 Hz, 2H), 1.79–1.72 (m, 2H), 1.34 (t, J = 6.63, 6.63 Hz, 2H), 1.29–1.22 (m, 4H); ^{13}C NMR (CDCl$_3$, 125 MHz) δ/ppm: 148.8, 138.3, 136.3, 134.3, 133.2, 128.2, 127.0, 124.8, 122.1, 121.7, 114.3, 40.2, 36.8, 27.0, 25.053, 22.4, 22.0; HRMS (ESI): C$_{17}$H$_{21}$N$_3$O$_2$S [M+Na]$^+$; calculated for 331.1354, found 354.1244.

benzyl(N-(quinolin-8-yl)sulfamide (**3i**) White powder, 47% yield, mp. 85–86 °C; IR: 3443, 3265, 2930, 1679, 1504, 1472, 1454, 1412, 1365, 1332, 1305, 1147, 1087, 1051, 925, 825, 791 cm^{-1}; ^{1}H NMR (CDCl$_3$, 500 MHz) δ/ppm: 8.68 (s, 1H), 8.08 (dd, J = 8.3, 1.6 Hz, 1H), 7.67 (dd, J = 6.8, 1.9 Hz, 1H), 7.44–7.41 (m, 2H), 7.39–7.36 (m, 1H),

7.01–6. 99 (m, 3H), 6.93–6.91 (m, 2H), 4.07 (d, $J = 5.3$ Hz, 2H); ^{13}C NMR (CDCl$_3$, 125 MHz) δ/ppm: 148.7, 138.3, 136.2, 135.9, 134.1, 128.5, 128.2, 127.8, 127.8, 126.9, 122.0, 121.7, 114.4, 47.3; HRMS (ESI): C$_{16}$H$_{15}$N$_3$O$_2$S [M+Na]$^+$; calculated for 313.0885, found 336.0775.

4-benzyl-*N*-(quinolin-8-yl)piperidine-1-sulfamide (**3j**) White powder, 29% yield, mp. 105–106 °C; IR: 3255, 2921, 1504, 1469, 1455, 1415, 1381, 1341, 1311, 1241, 1162, 1087, 1062, 1044, 926, 823, 791, 743, 719, 699, 640 cm^{-1}; ^{1}H NMR (CDCl$_3$, 500 MHz) δ/ppm: 8.82 (s, 1H), 8.70 (dd, $J = 4.21$, 1.64 Hz, 1H), 8.06 (dd, $J = 8.29$, 1.63 Hz, 1H), 7.69 (dd, $J = 6.68$, 2.19 Hz, 1H), 7.40–7.37 (m, 2H), 7.14 (dd, $J = 11.89$, 4.76 Hz, 2H), 7.12–7.04 (m, 1H), 6.93 (dd, $J = 13.77$, 6.78 Hz, 2H), 3.74 (d, $J = 12.27$ Hz, 2H), 2.57–2.52 (m, 2H), 2.31 (d, $J = 7.24$ Hz, 2H), 1.50–1.47 (m, 2H), 1.40–1.29 (m, 2H), 1.06–1.03 (m, 1H); ^{13}C NMR (CDCl$_3$, 125 MHz) δ/ppm: 148.7, 139.8, 138.3, 136.3, 134.6, 129.0, 128.3, 128.2, 126.9, 126.0, 122.0, 121.5, 115.0, 46.7, 42.6, 37.3, 31.3; HRMS (ESI): C$_{21}$H$_{23}$N$_3$O$_2$S [M+Na]$^+$; calculated for 381.1511, found 404.1401.

benzo[d][1,3]dioxol-5-yl-methyl(N-(quinolin-8-yl)sulfamide) (**3k**) Whitish powder, 37% yield, mp. 140–141 °C; IR: 3361, 3266, 1505, 1492, 1445, 1411, 1379, 1363, 1303, 1250, 1149, 1042, 925, 825, 757 cm^{-1}; ^{1}H NMR (CDCl$_3$, 500 MHz) δ/ppm: 8.89 (s, 1H), 8.71 (dd, $J = 4.19$, 1.61 Hz, 1H), 8.10 (dd, $J = 8.29$, 1.60 Hz, 1H), 7.66 (dd, $J = 6.37$, 2.45 Hz, 1H), 7.51–7.42 (m, 2H), 7.42–7.35 (m, 1H), 6.40 (t, $J = 7.9$ Hz, 2H), 6.36 (d, $J = 1.24$ Hz, 1H), 5.73 (s, 2H), 4.00 (d, $J = 5.87$ Hz, 2H); ^{13}C NMR (CDCl$_3$, 125 MHz) δ/ppm: 148.6, 147.6, 147.1, 138.2, 136.2, 134.1, 129.5, 128.2, 126.9, 122.0, 121.7, 121.4, 114.3, 108.3, 108.0, 101.0, 47.2; HRMS (ESI): C$_{17}$H$_{15}$N$_3$O$_4$S [M+Na]$^+$; calculated for 357.0783, found 380.0674.

3,4-dimethoxyphenethyl(N-(quinolin-8-yl)sulfamide) (**3l**) Whitish powder, 38% yield, mp. 116–117 °C; IR: 3328, 3292, 1592, 1579, 1504, 1458, 1438, 1409, 1353, 1332, 1314, 1236, 1146, 1102, 1024, 950, 913, 875, 819, 781 cm^{-1}; ^{1}H NMR (CDCl$_3$, 500 MHz) δ/ppm: 8.93 (s, 1H), 8.75 (dd, $J = 4.20$, 1.59 Hz, 1H), 8.11 (dd, $J = 8.28$, 1.55 Hz, 1H), 7.53 (dd, $J = 7.54$, 1.13 Hz, 1H), 7.44–7.40 (m, 2H), 7.39–7.32 (m, 1H), 6.57 (d, $J = 8.08$ Hz, 1H), 6.43–6.31 (m, 2H), 4.50 (s, 1H), 3.76 (s, 3H), 3.62 (s, 3H), 3.19 (s, 2H, br), 2.56 (t, $J = 6.68$ Hz, 2H); ^{13}C NMR (CDCl$_3$, 125 MHz) δ/ppm: 149.0, 148.7, 147.7, 138.2, 136.3, 134.1, 129.8, 128.2, 126.9, 122.0, 121.6, 120.5, 114.1, 111.4, 111.1, 55.8, 55.7, 44.2, 34.8; HRMS (ESI): C$_{19}$H$_{21}$N$_3$O$_4$S [M+Na]$^+$; calculated for 387.1253, found 410.1143.

4.3. CA inhibition assays

In order to determine the CA inhibition of the compounds, the method mentioned in the previous studies was used and inhibition results were obtained as described in refs. [29–34].

4.4. Cell cytotoxicity assay

The cytotoxicity of the test compounds on human colorectal adenocarcinoma cell line (HT-29; HTB-38), human breast adenocarcinoma cell line (MCF7; HTB-22), human prostate adenocarcinoma cell line (PC3; CRL-1435) and human healthy skin fibroblast cell line (CCD-986Sk; CRL-1947) were evaluated by MTT (3-(4,5 dimethylthiazol-2-yl)-2,5-diphenyltetrazolium bromide) assay according to described methods [8].

4.5. Docking studies

Three-dimensional structures of the investigated ligands were prepared with MOE (v2019.0102, Chemical Computing Group Inc., Montreal) in low-energy conformations. The most prevalent protonation state of the ligands at pH 7 was calculated. Subsequently, the ligands were energy minimized using the AM1 force field. The total procedure was implemented as described in our previous study [35].

All necessary hCA crystal structures were obtained from the Brookhaven Protein Data Bank, i.e. hCA I in complex with topiramate (pdb: 3lxe, 1.9 Å), hCA II in complex with 2,5-dihydroxybenzoic acid and a zinc-bound water molecule (pdb: 4e3d, 1.6 Å), hCA IX (pdb: 3iai, 2.2 Å) and hCA XII (pdb: 1jd0, 1.5 Å) both in complex with acetazolamide. The zinc-bound water molecule of the hCA II structure and all ligands (acetazolamide, topiramate and 2,5-dihydroxybenzoic acid) were retained and all other non-protein atoms were deleted from the crystal structures. Only chain A was retained if more than one protein structure was present. Hydrogen atoms were added with the "protonate 3D" [35] tool of the MOE software package and subsequently a steepest-descent energy minimization was performed using the AMBER14:EHT force field. The four protein structures were superposed on the backbone atoms of hCA I (Cα atoms, RMSD: 1.395 Å, for 236 residues). The coordinates of the hCA II zinc-bound water molecule were copied into the other hCA structures.

Docking studies were performed using the FlexX docking tool (v2.3.2; BioSolveIT GmbH, St. Augustin, Germany) within MOE. The binding pocket was described as all residues within 11 Å of the cocrystallized ligand. The highest scoring three poses were retained and analysed for complementarity between ligand and binding pocket with respect to sterics, interactions and electrostatics.

4.6. Molecular dynamics simulations

In this study, the Yasara Structure software package (v18.8.9, YASARA Biosciences GmbH) with the PME method was used for molecular dynamics simulations [36–38]. In the system prepared, the steepest-descent protocol (AMBER14) was used to minimize the energy [39,40]. The system was executed according to the whole procedure and all bonds were restricted using LINCS and SETTLE algorithms [41,42]. Snapshots were taken every 100 ps of the 10 ns production run. The binding energy (MM/PBSA) was calculated with Yasara Structure, while the RMSD values as well as the binding interactions (protein–ligand interaction fingerprint) were calculated with MOE.

Declaration of Competing Interest

The authors declare that they have no known competing financial interests or personal relationships that could have appeared to influence the work reported in this paper.

Acknowledgments

Appendix A. Supplementary data

^{1}H and ^{13}C NMR and MS spectra of the synthesized compounds and dose curve graphs of enzyme inhibition and controls are given in Supplementary Materials. Supplementary data to this article can be found online at https://doi.org/10.1016/j.bioorg.2021.104778.

References

[1] S. Akocak, O. Guzel-Akdemir, R. Kishore Kumar Sanku, S.S. Russom, B.I. Iorga, C.T. Supuran, M.A. Ilies, Pyridinium derivatives of 3-aminobenzenesulfonamide are nanomolar-potent inhibitors of tumor-expressed carbonic anhydrase isozymes CA IX and CA XII, Bioorg. Chem., 103, (2020), 104204.

[2] C.T. Supuran, Carbonic anhydrases: novel therapeutic applications for inhibitors and activators, Nat. Rev. Drug Discov. 7 (2) (2008) 168–181.

[3] V. Alterio, M. Hilvo, A. Di Fiore, C.T. Supuran, P. Pan, S. Parkkila, A. Scaloni, J. Pastorek, S. Pastorekova, C. Pedone, A. Scozzafava, S.M. Monti, G. De Simone, Crystal structure of the catalytic domain of the tumor-associated human carbonic anhydrase IX, Proc. Natl. Acad. Sci. USA 106 (38) (2009) 16233–16238.

[4] O.O. Guler, G. De Simone, C.T. Supuran, Drug design studies of the novel antitumor targets carbonic anhydrase IX and XII, Curr. Med. Chem. 17 (15) (2010) 1516–1526.

[5] D. Neri, C.T. Supuran, Interfering with pH regulation in tumours as a therapeutic strategy, Nat. Rev. Drug. Discov. 10 (10) (2011) 767–777.

[6] C.T. Supuran, Carbonic anhydrase inhibitors as emerging agents for the treatment and imaging of hypoxic tumors, Expert Opin. Investig. Drugs 27 (12) (2018) 963–970.

[7] A. Nocentini, C.T. Supuran, Advances in the structural annotation of human carbonic anhydrases and impact on future drug discovery, Expert Opin. Drug. Discov. 14 (11) (2019) 1175–1197.

[8] B. Zengin Kurt, F. Sonmez, D. Ozturk, A. Akdemir, A. Angeli, C.T. Supuran, Synthesis of coumarin-sulfonamide derivatives and determination of their cytotoxicity, carbonic anhydrase inhibitory and molecular docking studies, Eur. J. Med. Chem. 183 (2019) 111702.

[9] C.T. Supuran, Carbonic anhydrase inhibitors and their potential in a range of therapeutic areas, Expert Opin. Ther. Pat. 28 (10) (2018) 709–712.

[10] B.Z. Kurt, A. Dag, B. Dogan, S. Durdagi, A. Angeli, A. Nocentini, C.T. Supuran, F. Sonmez, Synthesis, biological activity and multiscale molecular modeling studies of bis-coumarins as selective carbonic anhydrase IX and XII inhibitors with effective cytotoxicity against hepatocellular carcinoma, Bioorg. Chem. 87 (2019) 838–850.

[11] B.Z. Kurt, F. Sonmez, S. Durdagi, B. Aksoydan, R.E. Salmas, A. Angeli, M. Kucukislamoglu, C.T. Supuran, Synthesis, biological activity and multiscale molecular modeling studies for coumaryl-carboxamide derivatives as selective carbonic anhydrase IX inhibitors, J. Enzyme Inhib. Med. Chem. 32 (1) (2017) 1042–1052.

[12] B.Z. Kurt, F. Sonmez, C. Bilen, A. Ergun, N. Gencer, O. Arslan, M. Kucukislamoglu, Synthesis, antioxidant and carbonic anhydrase I and II inhibitory activities of novel sulphonamide-substituted coumarylthiazole derivatives, J. Enzyme Inhib. Med. Chem. 31 (6) (2016) 991–998.

[13] C.T. Supuran, Coumarin carbonic anhydrase inhibitors from natural sources, J. Enzyme Inhib. Med. Chem. 35 (1) (2020) 1462–1470.

[14] A. Akincioglu, I. Gulcin, I. Kazaz, S. Durdagi, C.T. Supuran, S. Goksu, Discovery of potent carbonic anhydrase and acetylcholine esterase inhibitors: novel sulfamoylcarbamates and sulfamides derived from acetophenones, Bioorg. Med. Chem. 23 (13) (2015) 3592–3602.

[15] M.L. Villalba, P. Palestro, M. Ceruso, J.L. Gonzalez Funes, A. Talevi, L. Bruno Blanch, C.T. Supuran, L. Gavernet, Sulfamide derivatives with selective carbonic anhydrase VII inhibitory action, Bioorg. Med. Chem. 24 (4) (2016) 894–901.

[16] A. Akincioglu, Y. Akbaba, H. Gocer, S. Goksu, I. Gulcin, C.T. Supuran, Novel sulfamides as potential carbonic anhydrase isoenzymes inhibitors, Bioorg. Med. Chem. 21 (6) (2013) 1379–1385.

[17] L. Gavernet, J.L. Gonzalez Funes, P.H. Palestro, L.E. Bruno Blanch, G.L. Estiu, A. Maresca, I. Barrios, C.T. Supuran, Inhibition pattern of sulfamide-related compounds in binding to carbonic anhydrase isoforms I, II, VII, XII and XIV, Bioorg. Med. Chem. 21 (6) (2013) 1410–1418.

[18] J.Y. Winum, A. Scozzafava, J.L. Montero, C.T. Supuran, The sulfamide motif in the design of enzyme inhibitors, Expert Opin. Ther. Pat. 16 (1) (2006) 27–47.

[19] K. Aksu, M. Nar, M. Tanc, D. Vullo, I. Gulcin, S. Goksu, F. Tumer, C.T. Supuran, Synthesis and carbonic anhydrase inhibitory properties of sulfamides structurally related to dopamine, Bioorg. Med. Chem. 21 (11) (2013) 2925–2931.

[20] S. Goksu, A. Naderi, Y. Akbaba, P. Kalin, A. Akincioglu, I. Gulcin, S. Durdagi, R. E. Salmas, Carbonic anhydrase inhibitory properties of novel benzylsulfamides using molecular modeling and experimental studies, Bioorg. Chem. 56 (2014) 75–82.

[21] C.A. Costa, R.M. Lopes, L.S. Ferraz, G.N.N. Esteves, J.F. Di Iorio, A.A. Souza, I.M. de Oliveira, F. Manarin, W.A.S. Judice, H.A. Stefani, T. Rodrigues, Cytotoxicity of 4-substituted quinoline derivatives: anticancer and antileishmanial potential, Bioorg. Med. Chem. 28 (11) (2020).

[22] M.F. El Shehry, M.M. Ghorab, S.Y. Abbas, E.A. Fayed, S.A. Shedid, Y.A. Ammar, Quinoline derivatives bearing pyrazole moiety: synthesis and biological evaluation as possible antibacterial and antifungal agents, Eur. J. Med. Chem. 143 (2018) 1463–1473.

[23] M.M. Ghorab, F.A. Ragab, H.I. Heiba, R.K. Arafa, E.M. El-Hossary, In vitro anticancer screening and radiosensitizing evaluation of some new quinolines and pyrimido[4,5-b]quinolines bearing a sulfonamide moiety, Eur. J. Med. Chem. 45 (9) (2010) 3677–3684.

[24] M. Bozdag, A.M. Alafeefy, A.M. Altamimi, F. Carta, C.T. Supuran, D. Vullo, Synthesis of new 3-(2-mercapto-4-oxo-4H-quinazolin-3-yl)-benzenesulfonamides with strong inhibition properties against the tumor associated carbonic anhydrases IX and XII, Bioorg. Med. Chem. 25 (10) (2017) 2782–2788.

[25] V.K. Agrawal, S. Bano, C. Supuran, P.V. Khadikar, QSAR study on carbonic anhydrase inhibitors: aromatic/heterocyclic sulfonamides containing 8-quinoline-sulfonyl moieties, with topical activity as antiglaucoma agents, Eur. J. Med. Chem. 39 (7) (2004) 593–600.

[26] B.S. Huang, W.M. Chen, T. Zhao, Z.Y. Li, X.Y. Jiang, T. Ginex, D. Vilchez, F. J. Luque, D.W. Kang, P. Gao, J. Zhang, Y. Tian, D. Daelemans, E. De Clercq, C. Pannecouque, P. Zhan, X.Y. Liu, Exploiting the Tolerant Region I of the Non-Nucleoside Reverse Transcriptase Inhibitor (NNRTI) binding pocket: discovery of potent diarylpyrimidine-typed HIV-1 NNRTIs against wild-type and E138K mutant virus with significantly improved water solubility and favorable safety profiles, J. Med. Chem. 62 (4) (2019) 2083–2098.

[27] M.H. Bolli, C. Boss, C. Binkert, S. Buchmann, D. Bur, P. Hess, M. Iglarz, S. Meyer, J. Rein, M. Rey, A. Treiber, M. Clozel, W. Fischli, T. Weller, The discovery of N-[5-(4-Bromophenyl)-6-[2-[(5-bromo-2-pyrimidinyl)oxy]ethoxy]-4-pyrimidinyl]-N '-propylsulfamide (Macitentan), an orally active, potent dual endothelin receptor antagonist, J. Med. Chem. 55 (17) (2012) 7849–7861.

[28] K.C. Nicolaou, D.A. Longbottom, S.A. Snyder, A.Z. Nalbanadian, X.H. Huang, A new method for the synthesis of nonsymmetrical sulfamides using Burgess-type reagents, Angew. Chem. Int. Edit. 41 (20) (2002) 3866–3870.

[29] R.G. Khalifah, The carbon dioxide hydration activity of carbonic anhydrase. I. Stop-flow kinetic studies on the native human isoenzymes B and C, J. Biol. Chem. 246 (8) (1971) 2561–2573.

[30] S. Angapelly, P.V.S. Ramya, A. Angeli, C.T. Supuran, M. Arifuddin, Sulfocoumarin-, coumarin-, 4-sulfamoylphenyl-bearing indazole-3-carboxamide hybrids: synthesis and selective inhibition of tumor-associated carbonic anhydrase isozymes IX and XII, Chemmedchem. 12 (19) (2017) 1578–1584.

[31] K. Tars, D. Vullo, A. Kazaks, J. Leitans, A. Lends, A. Grandane, R. Zalubovskis, A. Scozzafava, C.T. Supuran, Sulfocounnarins (1,2-benzoxathiine-2,2-dioxides): a class of potent and isoform-selective inhibitors of tumor-associated carbonic anhydrases, J. Med. Chem. 56 (1) (2013) 293–300.

[32] A. Grandane, M. Tanc, R. Zalubovskis, C.T. Supuran, Synthesis of 6-aryl-substituted sulfocoumarins and investigation of their carbonic anhydrase inhibitory action, Bioorg. Med. Chem. 23 (7) (2015) 1430–1436.

[33] A. Bonardi, M. Falsini, D. Catarzi, F. Varano, L.D. Mannelli, C. Tenci, C. Ghelardini, A. Angeli, C.T. Supuran, V. Colotta, Structural investigations on coumarins leading to chromeno[4,3-c] pyrazol-4-ones and pyrano[4,3-c]pyrazol-4-ones: New scaffolds for the design of the tumor-associated carbonic anhydrase isoforms IX and XII, Eur. J. Med. Chem. 146 (2018) 47–59.

[34] E. Berrino, M. Bozdag, S. Del Prete, F.A.S. Alasmary, L.S. Alqahtani, Z. AlOthman, C. Capasso, C.T. Supuran, Inhibition of alpha-, beta-, gamma-, and delta-carbonic anhydrases from bacteria and diatoms with N'-aryl-N-hydroxy-ureas, J. Enzyme Inhib. Med. Chem. 33 (1) (2018) 1194–1198.

[35] P. Labute, Protonate3D: assignment of ionization states and hydrogen coordinates to macromolecular structures, Proteins 75 (1) (2009) 187–205.

[36] E. Krieger, G. Vriend, New ways to boost molecular dynamics simulations, J. Comput. Chem. 36 (13) (2015) 996–1007.

[37] E. Krieger, G. Vriend, YASARA View - molecular graphics for all devices - from smartphones to workstations, Bioinformatics 30 (20) (2014) 2981–2982.

[38] L.P. Ulrich Essmann, Max L. Berkowitz, A smooth particle mesh Ewald method, J. Chem. Physic. 103 (1995) 8577–8593.

[39] J.A. Maier, C. Martinez, K. Kasavajhala, L. Wickstrom, K.E. Hauser, C. Simmerling, ff14SB: improving the accuracy of protein side chain and backbone parameters from ff99SB, J. Chem. Theory. Comput. 11 (8) (2015) 3696–3713.

[40] V. Hornak, R. Abel, A. Okur, B. Strockbine, A. Roitberg, C. Simmerling, Comparison of multiple Amber force fields and development of improved protein backbone parameters, Proteins 65 (3) (2006) 712–725.

[41] B. Hess, H. Bekker, H.jC. Berendsen, J.G.E. Fraaije, LINCS: a linear constraint solver for molecular simulations, J. Comput. Chem. 18 (12) (1997) 1463–1472.

[42] S. Miyamoto, P.A. Kollman, Settle: an analytical version of the SHAKE and RATTLE algorithm for rigid water models, J. Comput. Chem. 13 (8) (1992) 952–962.